Revista Brasileira de Física, Vol. 5, N.º 2, 1975

Nuclear Quadrupole Resonance in $CuCl_2.2H_2O$

Y. S. LIU and L. T. Peixoto*

Departamento de Física, Universidade de Brasília, Brasília, D.F

Recebido em 27 de Fevereiro de 1975

The electric field gradient (EFG) at the Cl^- site of $CuCl_2 . 2H_2O$ has been calculated on the basis of a point charge model plus the contribution of the covalent bond between nearest copper and chlorine ions. In the calculations of the EFG at Cu^{++} site, it has been included the contribution of the $3d^9$ electrons in the valence shell of copper and neglected the effect of chemical bonding. After comparison with experimental NOK results, it has been discussed the shielding effect of the core electrons of both ions and established values for the so called Sternheimer factors. It has also been presented a value for the ionicity of chlorine in the crystal and calculated the temperature dependence of the quadrupole splitting of the copper nucleus.

O gradiente de campo elétrico (EFG) na posição do íon Cl^- no composto $CuCl_2 . 2H_2O$ foi calculado com base em um modelo de carga pontual acrescido do efeito da ligação covalente do íon de cobre com o íon de cloro mais próximo. No cálculo do EFG na posição do ion Cu^{++} foi incluída a contribuição dos elétrons $3d^9$ na camada de valência do cobre e ignorado o efeito da ligação química. Efetuada a comparação com resultados experimentais obtidos com NQR, foi discutido o efeito de blindagem provocado pelos elétrons do cerne em ambos os íons e estabelecidos valores para os denominados fatores de Sternheimer. Foi ainda apresentado um valor para a ionicidade do cloro no cristal e calculada e dependência com a temperatura do desdobramento quadrupolar do núcleo de cobre.

1. Introduction

The Sternheimer factor γ_∞ of Cl^- was calculated as -27 by Burns and Wikner[1], who used contracted wave functions. Liu[2], seeking for a theoretical result compatible with NQR measurements on monocrystalline $CoCl_2 . 2H_2O$, found $\gamma_\infty = -31$. The calculation of this author was carried upon a point charge model and had taken into account the effect of covalent bond of the Cl^- ion with the two nearest Co^{++} ions and had led to an ionicity of 91.1% for the chlorine in the compound. In our investigation of the factor γ_∞ of Cl^-, we have considered the monocrystal of $CuCl_2 . 2H_2O$ and adopted the same model of Liu but neglecting one of the two Cu-C1 bonding which is 30% longer.

*Present address: Instituto de Física "Gleb Wataghin", Campinas SP.

To calculate the Sternheimer factors γ_∞ and R of Cu^{++}, we have also considered the compound $CuCl_2.2H_2O$ and adopted a method which gives the results in dependence of the accepted value of $\langle r^{-3}\rangle_{3d}$. Morgan and Wolney[3], calculating the EFG at the Cu site of $CuBr_2$ have considered oniy the valence contribution and found that, when taking R = 0, the value $\langle r^{-3}\rangle_{3d} = 2.8$ a.u. is the best account for experimental results. Introducing the crystalline contribution via a point charge model. Liu[4] has taken $\gamma_\infty = -11$ (Ref. 5) and expressed the conclusion that the value R = 0.52 agrees as much as the value $\langle r^{-3}\rangle_{3d} = 8.252$ a.u., generally accepted for the ion Cu^{++}, as the measured NQK absorption frequency. Our calculation is based upon the same model of Liu and seems to point out that the values $\gamma_\infty = -11$, R = 0.57 and $\langle r^{-3}\rangle_{3d} = 8.252$ a.u. are compatible to each other and with experimental results.

2. Theory

The EFG at Cl site can be written as

$$V_{ij}(Cl) = i(1-\gamma_\infty)V_{ij}^{PC} + (1-i)V_{ij}^{B}, \tag{1}$$

where i is the ionicity. The first term represents the contribution of the point charges at the crystalline sites while the second arises from the charge distribution envolved in the Cu-Cl bonding. These can be expressed as

$$V_{ij}^{PC} = \sum_k \frac{q_k}{r_k^5}\,(3x_i^{(k)}x_j^{(k)} - r_k^2\,\delta_{ij}), \tag{2}$$

$$V_{ij}^{B} = (1-s^2)\;q_{at}\sum_k \frac{1}{r_k^2}\,(3x_i^{(k)}x_j^{(k)} - r_k^2\,\delta_{ij}). \tag{3}$$

In the last expression. q_{at} is the main EFG component at the nucleus of chlorine. supposed a free atom and $s^2 = 0.15$ indicates the s-character of the bonding electrons.

Thc EFG at Cu site can be written as

$$(\;C\;) = (1\quad R)\;V_{ij}^{val} + (1-\gamma_\infty)\;V_{ij}^{PC}. \tag{4}$$

The first term is due to the $3d^y$ valence electrons and the second, to the crystalline point charges. The contribution of chemical bonding is neglected because it is predicted a high ionicity of the copper.

The components V_{ij}^{val} can be calculated by considering the hole in the 3d shell of Cu^{++}. The energy levels and corresponding wavefunctions are determined by the Hamiltonian:

$$H = e \sum_{l,m} \frac{4\pi}{2l+1} q_l^m \, r^{-(l+1)} Y_l^m \, (\theta, \phi) + \lambda \, \mathrm{L.S}, \tag{5}$$

where λ is the spin-orbit coupling constant, taken as -830 cm^{-1}, and q_l^m are the electric multipole moments of the crystalline point charge distribution:

$$q_l^m = \sum_k q_k \, r_k^l \, Y_l^{m*} \, (\theta_k, \phi_k). \tag{6}$$

The hole has orbital angular momentum 2 and spin 1/2, so that the Hamiltonian is represented by a 10 x 10 hermitian matrix whose diagonalization leads to the desired energy levels and corresponding eigenfunctions.

The EFG components due to the n^{th} eigenfunction is given by

$$V_{ij}^{val}(n) = \int |\psi_n|^2 \, \frac{3x_i x_j - r^2 \delta_{ij}}{r^5} \, d^3r, \tag{7}$$

so that the statistical average at temperature T is calculated by

$$V_{ij}^{val} = \frac{\sum_{n=1}^{10} V_{ij}^{val}(n) \exp|-E(n)/kT|}{\sum_{n=1}^{10} \exp|-E(n)/kT|}. \tag{8}$$

Once the various components of the total EFG tensor at Cl or Cu nucleus are found, we diagonalize the corresponding matrix to find now the principal components of that tensor. The matrix of the eigenvectors now contains the direction cosines that relates the principal EFG axis to the crystalline axis. The quadrupolar splitting energy is given by

$$\Delta E = \frac{e^2 qQ}{2} \sqrt{1 + \eta^2/3}, \tag{9}$$

where the so-called asymetry parameter η and the "electric-field gradient" eq are well defined in terms of the principal EFG components. Q is the electric quadrupole moment of the nucleus.

3. Experimentals

The NQR absorption frequency of chlorine in $CuCl_2 . 2H_2O$ is well known as 9.05 MHz at room temperature. We have used a super--regenerative NQR spectrometer of the *Universidade de Brasilia* to measure the absorption frequencies of the isotopes ^{63}Cu and ^{65}Cu in the same crystal. A series of spectra we have taken shows three absorption lines at 28.68 ± 0.03 MHz, 28.52 ± 0.03 MHz and 26.78 ± 0.06 MHz (Fig. 1), the relative intensity of the first and the last of which is nearly equal to the relative natural abundance of the isotopes ^{63}Cu and ^{65}Cu (69% and 31%, respectively). Also, the ratio of the corresponding frequencies are nearly the same as that of the quadrupole moments $Q = 0.157$ barns and $Q = 0.145$ barns of the isotopes ^{63}Cu and ^{65}Cu, respectively. Since the environment of different copper nucleus in $CuCl_2 . 2H_2O$ are identical, the above ratio would be predicted by Eq. (9), so leading our conclusion that 28.68 MHz and 26.78 MHz are nearly the frequencies we have been seeking for.

In order to explain the intermediate line, we have considered various hypotheses, some of which have been discarded by virtue of the absence of a fourth line at approximately 26.62 MHz and some others because are in conflict with the purity specifications of the sample used. We have also applied magnetic fields of different intensities between 50 Gauss and 150 Gauss to investigate the hypothesis of a Zeeman splitting of the quadrupolar lines produced by ^{63}Cu and ^{65}Cu. In view of the negative results, we think that the explanation must arise from a repetition of the experiment under a severe chemical control.

4. Theoretical Results and Discussion

The structure of $CuCl_2 . 2H_2O$ is orthorhombic, bimolecular, with $a_0 = 7.38$ Å, $b_0 = 8.04$ Å and $c_0 = 3.72$ Å. The crystalline sites are at:

$$\text{Cu:} \quad \left(0, 0, 0; \frac{1}{2}, \frac{1}{2}, 0\right),$$

$$\text{Cl:} \pm \left(u, 0, v; \frac{1}{2} - u, \frac{1}{2}, -v\right),$$

$$\text{O:} \pm \left(0, w, 0; \frac{1}{2}, \frac{1}{2} + w, 0\right),$$

$$H:\ \pm\left(x, y, z;\ x, -y, z;\ \frac{1}{2}+x, \frac{1}{2}+y, -z;\ \frac{1}{2}-x, \frac{1}{2}+y, z\right),$$

where $u = 0.24$, $v = 0.38$, x = 0.082, $y = 0.307$, $z = 0.130$ and w = 0.239. The adopted electric charges were $+2\,|e|$ for Cu, $-|e|$ for Cl, $-0.70\,|e|$ for O and $+0.35\,|e|$ for H. Fig. 2 shows a segment of the Cu-Cl chain parallel to the c axis, in which each ion Cu^{++} is surrounded by four Cl^- ions. Two water molecules on the b axis, above and below the ion Cu^{++}, complete a distorted octahedral symmetry around each copper ion.

The summation over the crystalline sites to find the EFG at the Cl^- ion was performed according to two idependently coded programs in a PDP-11 and a IBM 1130 computers of the Universidade de Brasilia. It was considered the ions inside a sphere of radius 30 Å centered at a Cl^- site. Fig. 3 shows the calculated NQR frequencies as functions of $(1 - y,)$ for different values of the ionicity. There are two pairs of values (i, γ_∞) compatible with the measured values y = 0.42 (Ref. 6) and v = 8.96 MHz of the asymmetry parameter and NQR frequency: (0.7122,– 26.8101) and (0.9244, 22.0777). In Fig. 4 they are obtained by the interception of the plane $\eta = 0.42$ with the three-dimensional plotted curves. Our result $\gamma_\infty = -26.8101$ is very near to that found by Burns and Wikner[1] and through the corresponding direction cosines in Table I determines the principal axis configuration of Fig. 5, where the x principal axis coincides with the crystalline axis b.

	i = 0.7122 $1-\gamma_\infty$ = 27.8101	i = 0.9244 $1-\gamma_\infty$ = –21.0777	Experiments	Sullivan *et* al.
V_{xx}	0.0650 (0, 1, 0)	–0.0651 (–0.5949,0,0.8038)	–0.065 (–0.595,0,0.803)	–0.02287 (0.537,0, 0.843)
V_{yy}	0.1596 (–0.6522,0,0.7581)	–0.1596 (0, 1, 0)	–0.160 (0, 1, 0)	–0.15428 (0, 1, 0)
V_{zz}	–0.2247 (–0.7581,0,–0.6522)	0.2247 (0.8038,0,0.5949)	0.225 (0.803,0,0.0595)	0.17715 (0.843,0, 0.537)
η	0.42	0.42	0.42	0.74

Table I – Principal values (in units of $Å^{-3}$) of the EFG tensor at a Cl site in $CuCl_2.2H_2O$. The direction cosines of $V'_{,}, V_{yy}$ and V_{zz} given in brackets are measured with respect to the *a*, b and c crystal axis, respectively.

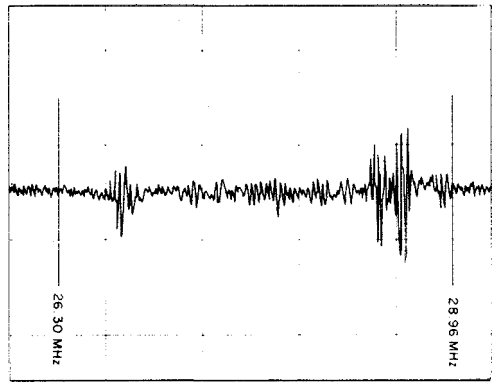

Fig. 1 – NQR spectrum of $CuCl_2 . 2H_2O$ between 26 MHz and 29 MHz.

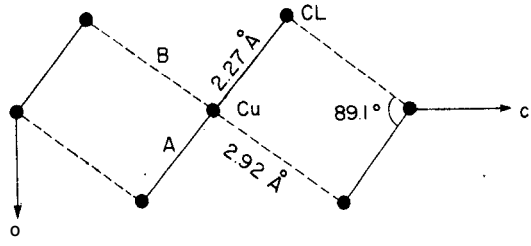

Fig. 2 – Polimeric chain Cu–Cl in the crystalline plane $a-c$ of $CuCl_2 . 2H_2O$.

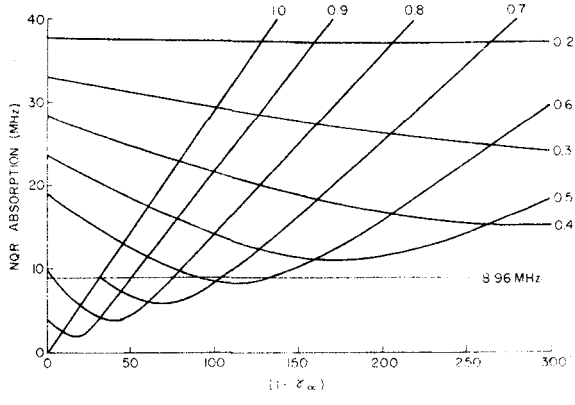

Fig. 3 – Theoretical curves of the NQR frequency versus $(1 - \gamma_\infty)$ for different values of the ionicity.

From Table I, one sees that the calculated direction cosines of the EFG tensor in best agreement with the experimental values of O'Sullivan *et al*[6] are those derived from i = 0.9244 and $\gamma_\infty = 22.0777$. This suggests that q_{at} may be positive rather than – 39.93, for in that case γ_∞ corresponding to i = 0.9244 would be – 20.0777, as can be seen from Eq. (1). Indeed, from the theory of Townes and Dailey, one can deduce that the principal values of the EFG at the Cl site along the o-bond is[9]

$$q = |(1-i)(1-s^2) + d^2(1+i)|\, e(1-R) \int |f(r)P_z|^2 \, \frac{3\cos^2\theta - 1}{r^3}\, d^3r,$$

where s and d are the amount of s and d hybridization in the bonding, R is a shielding factor, $0 < R < 1$. Taking $P_z = \sqrt{\frac{3}{4\pi}}\cos\theta$ and neglecting d^2, one has

$$q \simeq (1+i)(1-s^2)\, \frac{4}{5}\, e\langle 1/r^3\rangle\, (1-R).$$

Hence. one sees that q_{at} of Eq. *(3)* is equal to $4\langle 1/r^3\rangle (1-R)/5$ and is positive. Also, from thc table given by Das and Hahn[9], $e^2q_{at}Q = -109.746 \pm 0.01$ MHz, $Q = -0.07894 \pm 0.00002$ barns, one can also deduce that q_{at} must be positive.

Appendix I presents the Hamiltonian matrix of the hole of Cu^{++}. The so-called electrical multipole moments of the point charge distribution are given by

$$A_2^m = \frac{\sqrt{4\pi}}{7}\, |e|\, \frac{\sqrt{5}}{5}\, \langle r^2\rangle\, q_2^m,$$

$$A_4^m = \frac{\sqrt{4\pi}}{7}\, |e|\, \frac{1}{9}\, \langle r^4\rangle\, q_4^m.$$

The summation involved in the calculation of these multipole moments and the posterior diagonalization of the matrix was performed in the same computers with two independently coded programs. Taking into account the ions inside a sphere of radius 30 Å, centered at a Cu^{++} site and taking $(r^2) = 1.028$ a.u. and $(r^4) = 2.498$ a.u. (Ref. 7), we have the results for the multipole moments of tables II and III. The diagonalization of the matrix was performed under successive unitary transformations and have resulted in the five doubly-degenerate energy levels of Fig. 6. The first excited level is ahout 1176 cm^{-1} above

A_4^0	$\mathrm{Re}(A_4^1)$	$\mathrm{Im}(A_4^1)$	$\mathrm{Re}(A_4^2)$	$\mathrm{Im}(A_4^2)$	$\mathrm{Re}(A_4^3)$	$\mathrm{Im}(A_4^3)$	$\mathrm{Re}(A_4^4)$	$\mathrm{Im}(A_4^4)$
5.2624	−5.1984	0	−39.7432	0	15.0636	0	−34.8588	0

Table II – Values of the multipole moments A_4^m (in units of cm^{-1}) at the Cu site.

A_2^0	$\mathrm{Re}(A_2^1)$	$\mathrm{Im}(A_2^1)$	$\mathrm{Re}(A_2{}^2)$	$\mathrm{Im}(A_2^2)$
310.260	251.126	0	64.8168	0

Table III – Values of the multipole moments A_2^m (in units of cm^{-1}) at the Cu site.

the ground state level, leading to the conclusion that the EFG is almost entirely due to the degenerate ground states in the interval between 0°K and room temperature. Table IV presents the ten coefficients determining the state vector of each of the two ground states; one state vector results from the other by application of the time reversal operator $T = i\sigma_y k$, satisfying Kramer's theorem.

M_1	+2		+1		0		−1		−2	
M_s	+1/2	−1/2	+1/2	−1/2	+1/2	−1/2	+1/2	−1/2	+1/2	−1/2
$\psi^{(9)}$	−0.80620	0.21611	0.42064	−0.13479	−0.20896	0.00263	−0.10620	−0.03548	−0.19953	0.1154
$\psi^{(10)}$	−0.11054	−0.19953	−0.03548	0.10619	−0.00263	−0.20896	−0.13479	−0.42064	−0.21611	−0.80620

Table IV – The two-degenerate ground state wavefunctions of the $3d^9$ electron of Cu^{++} in terms of $Y_2^m \alpha_{\mathrm{spin}}$

Fig. 7 contains the theoretical curves of the NQR frequency versus temperature for the copper nucleus. The calculated values at room temperature $f_1 = 28.60$ MHz for ^{63}Cu and $f_2 = 26.80$ for ^{65}Cu, result when we take $\gamma_\infty = 11.5$ and $R = 0.57$. The assumed value $\langle r^{-3} \rangle_{3d} = 8.252$

a.u. (Ref. 7) is that of the free Cu^{++} ion. If we admit that in the body of the crystal a more realistic value is 0.8 of that for free ion[8], then $R = 0.48$ will become the correct shielding factor when f_1, f_2 and γ_∞ have the same values given above. On the other hand, if we modify γ_∞ by 20% and keep R constant, the new f_1 and f_2 values will be different less than 4% of the original ones. This shows that the total EFG depends almost entirely of the electronic contribution

Appendix I

We present below the 10 x 10 Hamiltonian matrix of the hole in the 3d shell of Cu^{++}. Each element is a result of the development of the expression (5) between appropriate basic states.

	$+2\ +\frac{1}{2}$	$+2\ -\frac{1}{2}$	$+1\ +\frac{1}{2}$	$+1\ -\frac{1}{2}$	$0\ +\frac{1}{2}$	$0\ -\frac{1}{2}$	$-1\ +\frac{1}{2}$	$-1\ -\frac{1}{2}$	$-2\ +\frac{1}{2}$	$-2\ -\frac{1}{2}$
$+2\ +\frac{1}{2}$	$-2A_2^0 + A_4^0 + \lambda$	0	$\sqrt{6}A_2^1 - \sqrt{5}A_4^1$	0	$-2A_2^2 + \sqrt{15}A_2^2$	0	$-\sqrt{35}A_4^3$	0	$\sqrt{70}A_4^4$	0
$+2\ -\frac{1}{2}$	0	$-2A_2^0 + A_4^0 - \lambda$	λ	$\sqrt{6}A_2^1 - \sqrt{5}A_4^1$	0	$-2A_2^2 - \sqrt{15}A_1^2$	0	$-\sqrt{35}A_1^3$	0	$\sqrt{70}A_4^4$
$+1\ +\frac{1}{2}$	$-\sqrt{6}A_2^1 + \sqrt{5}A_4^{-1}$	λ	$A_2^0 - 4A_4^0 + \lambda/2$	0	$A_2^1 + \sqrt{30}A_4^1$	0	$-\sqrt{6}A_2^2 - 2\sqrt{10}A_4^2$	0	$\sqrt{35}A_4^3$	0
$+1\ -\frac{1}{2}$	0	$-\sqrt{6}A_2^1 + \sqrt{5}A_4^{-1}$	0	$A_2^0 - 4A_4^0 - \lambda/2$	$6\lambda/2$	$A_2^1 - \sqrt{30}A_4^1$	0	$-\sqrt{6}A_2^2 - 2\sqrt{10}A_4^2$	0	$\sqrt{35}A_4^3$
$0\ +\frac{1}{2}$	$-2A_2^{-2} + \sqrt{15}A_4^{-2}$	0	$-A_2^{-1} - \sqrt{30}A_4^{-1}$	$\sqrt{6}\lambda/2$	$2A_2^0 + 6A_4^0$	0	$-A_2^1 - \sqrt{30}A_4^1$	0	$-2A_2^2 + \sqrt{15}A_4^2$	0
$0\ -\frac{1}{2}$	0	$-2A_2^{-2} + \sqrt{15}A_4^2$	0	$+A_2^{-1} + \sqrt{30}A_4^1$	0	$2A_2^0 + 6A_4^0$	$\sqrt{6}\lambda/2$	$-A_2^1 - \sqrt{30}A_4^1$	0	$-2A_2^2 + \sqrt{15}A_4^2$
$-1\ +\frac{1}{2}$	$\sqrt{35}A_4^3$	0	$-\sqrt{6}A_2^2 - 2\sqrt{10}A_4^2$	0	$A_2^{-1} + \sqrt{30}A_4^{-1}$	$\sqrt{6}\lambda/2$	$A_2^0 - 4A_4^0 - \lambda/2$	0	$-\sqrt{6}A_2^1 - \sqrt{5}A_4^1$	0
$-1\ -\frac{1}{2}$	0	$\sqrt{35}A_4^{-3}$	0	$-\sqrt{6}A_2^{-2} - 2\sqrt{10}A_4^{-2}$	0	$A_2^1 + \sqrt{30}A_4^{-1}$	0	$A_2^0 - 4A_1^0 + \lambda/2$	λ	$-\sqrt{6}A_2^1 + \sqrt{5}A_4^1$
$-2\ \frac{1}{2}$	$\sqrt{70}A_4^4$	0	$-\sqrt{35}A_4^3$	0	$-2A_2^2 + \sqrt{15}A_4^{-2}$	0	$\sqrt{6}A_2^{-1} - \sqrt{5}A_4^{-1}$	λ	$-2A_2^0 + A_4^0 - \lambda$	0
$-2\ -\frac{1}{2}$	0	$\sqrt{70}A_4^4$	0	$-\sqrt{35}A_4^3$	0	$-2A_2^2 + \sqrt{15}A_4^{-2}$	0	$\sqrt{6}A_2^{-1} - \sqrt{5}A_4^{-1}$	0	$-2A_2^0 + A_4^0 + \lambda$

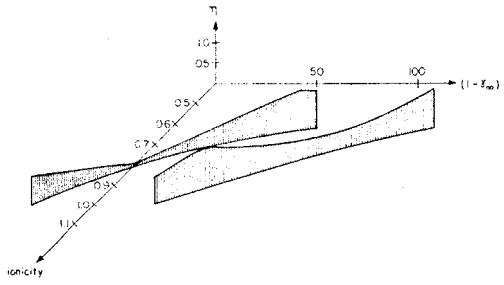

Fig. 4 – Three-dimensional plot of the asymmetry factor η of chlorine versus ionicity and $(1 - y_i)$.

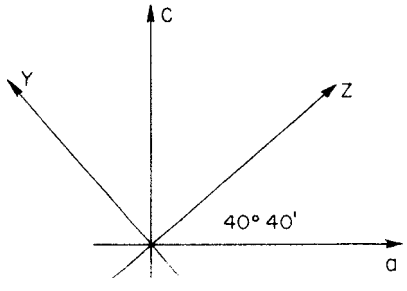

Fig. 5 – Configuration of the EFG principal axis of the Cl ion.

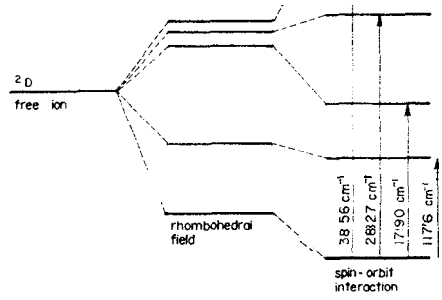

Fig. 6 – Energy levels diagram of the hole in the 3d shell of Cu^{++}

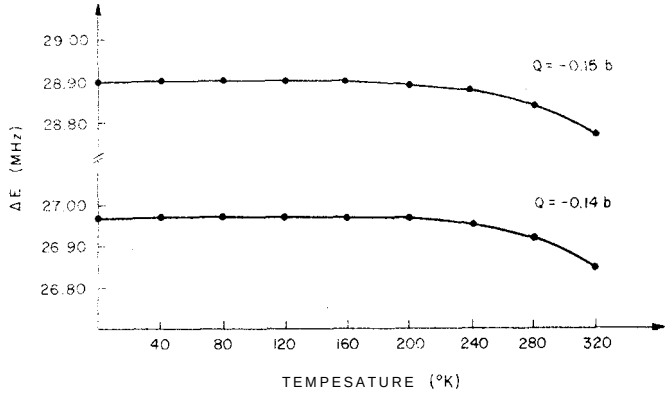

Fig. 7 – Temperature dependence of the quadrupole splitting of the copper nucleus.

Appendix II

We give below extended expressions of V_{ij}^{val} that result from Eq. (7). The C's are the coefficients of the spin-independent state vector $\psi = \sum_m C_m Y_2^m$ for the hole in the 3d shell of Cu^{++}.

$$V_{xx} = -\frac{2e}{7}\langle r^{-3}\rangle \left[|C_0|^2 + \frac{1}{2}(|C_1|^2 + |C_{-1}|^2) - (|C_{-2}|^2) + \sqrt{6}\,\mathrm{Re}\,(C_2^* C_0 + C_0^* C_{-2}) - 3\,\mathrm{Re}\,(C_1^* C_{-1}) \right]$$

$$V_{yy} = -\frac{2e}{7}\langle r^{-3}\rangle \left[|C_0|^2 + \frac{1}{2}(|C_1|^2 + |C_{-1}|^2) - (|C_{-2}|^2) - \sqrt{6}\,\mathrm{Re}\,(C_2^* C_0 + C_0^* C_{-2}) - 3\,\mathrm{Re}\,(C_1^* C_{-1}) \right]$$

$$V_{zz} = -\frac{2e}{7}\langle r^{-3}\rangle [-2|C_0|^2 - (|C_1|^2 + |C_{-1}|^2 + 2(|C_2|^2 - |C_{-2}|^2)]$$

$$V_{xy} = -\frac{2e}{7}\langle r^{-3}\rangle [-3\,\mathrm{Im}\,(C_1 C_{-1}^*) + \sqrt{6}\,\mathrm{Im}\,(C_2 C_0^* + C_0^* C_{-2})]$$

$$V_{xz} = -\frac{2e}{7}\langle r^{-3}\rangle \left[3\,\mathrm{Re}\,(C_2^* C_1 - C_{-1}^* C_{-2}) + \sqrt{\frac{3}{2}}\,\mathrm{Re}\,(C_1^* C_0 - C_0^* C_{-1}) \right]$$

$$V_{yz} = -\frac{2e}{7}\langle r^{-3}\rangle \left[3\,\mathrm{Im}\,(C_2^* C_1 - C_{-1}^* C_{-2}) + \sqrt{\frac{3}{2}}\,\mathrm{Im}\,(C_1^* C_0 - C_0^* C_{-1}) \right].$$

References

1. G. Burns and E. K. Wikner, Phys. Rev. 121, 155(1961).
2. Y. S. Liu, to be published in J. Chem. Phys. .
3. P. Morgen and W. Wolney Filho, preprint.
4. Y. S. Liu, submitted to publication.
5. L. T. Peixoto, M. Sc. Thesis, Departamento de Física, Universidade de Brasília.
6. W. J. O'Sullivan, Phys. Rev. 140 A, 1759(1969).
7. Abragam and Bleaney, *Electron Paramagnetic Resonance of Transition Ions*, Clarendon Press, pag. 399.
8. R. Ingalls, Phys. Rev. **133**, 3A, A787(1964).
9. T. P. Das and E. L. Hahn., *Solid State Physics. Supplement I-Nuclear Quadrupole Resonance Spectroscopy* (Acad. Press. New York – London) pp 120-179(1958).